ACS APPLIED MATERIALS & INTERFACES

Article

A Capacitive Pressure Sensor with High Sensitivity and Fast Response to Dynamic Interaction Based on Graphene and Porous Nylon Networks

Zhongfu He, Wenjun Chen, Binghao Liang, Changyong Liu, Leilei Yang, Dongwei Lu, Zichao Mo, Hai Zhu, Zikang Tang, and Xuchun Gui

ACS Appl. Mater. Interfaces, **Just Accepted Manuscript** • DOI: 10.1021/acsami.8b01050 • Publication Date (Web): 27 Mar 2018

ACS Publications

ACS Applied Materials & Interfaces is published by the American Chemical Society. 1155 Sixteenth Street N.W., Washington, DC 20036

A Capacitive Pressure Sensor with High Sensitivity and Fast Response to Dynamic Interaction Based on Graphene and Porous Nylon Networks

Zhongfu He [1,#], Wenjun Chen[1,#], Binghao Liang[1], Changyong Liu[2], Leilei Yang[1], Dongwei Lu[1], Zichao Mo[1], Hai Zhu[3], Zikang Tang[4], Xuchun Gui[1,*]

[1]*State Key Laboratory of Optoelectronic Materials and Technologies, School of Electronics and Information Technology, Sun Yat-sen University, Guangzhou, 510275, China*

[2]*Additive Manufacturing Research Institute, College of Mechatronics and Control Engineering, Shenzhen University, Shenzhen 518060, China*

[3]*State Key Laboratory of Optoelectronic Materials and Technologies, School of Physics, Sun Yat-Sen University, Guangzhou 510275, China*

[4]*Institute of Applied Physics and Materials Engineering, University of Macau, Avenida da Universidade, Taipa, Macau, China*

# These authors contributed equally to this work

*To whom correspondence should be addressed. E-mail: guixch@mail.sysu.edu.cn

Abstract

Flexible pressure sensors are of great importance to be applied in artificial intelligence and wearable electronics. However, assembling a simple structure, high performance capacitive pressure sensor, especially for the monitoring of the flow of liquid, is still a big challenge. Here, based on a sandwich-like structure, we propose a facile capacitive pressure sensor optimized by a flexible, low-cost nylon netting, showing many merits including high response sensitivity (0.33 kPa^{-1}) in a low-pressure regime (< 1 kPa), ultralow detection limit as 3.3 Pa, excellent working stability after more than 1000 cycles, and synchronous monitoring for human pulses and clicks. More important, this sensor exhibits ultrafast response speed (<20 ms), which enables its detection for the fast variations of a small applied pressure from the morphological changing processes of a falling droplet onto the sensor. Furthermore, a capacitive pressure sensor array is fabricated for demonstrating the ability to spatial pressure distribution. Our developed pressure sensors show great prospect in practical applications such as health monitoring, flexible tactile devices and motion detection.

Keywords: graphene; capacitive pressure sensor; flexible electronics; sandwich-like structure; nylon netting

1. Introduction

Flexible sensors are widely applied in electronic skins,[1-2] biomedical diagnostics,[3-5] human-health monitoring, motion detection[6-7] and wearable devices.[8-9] In recent, types of sensors including piezo-capacitive,[10-14] piezoresistive,[7,15-18] piezoelectric,[19-20] field-effect transistor (FET)[21-22] and trielectronic[23-24] sensors have been constructed for compression detection. Particularly, flexible pressure sensors based on capacitance effect are characterized by low energy consumption, excellent stability and fast dynamic response.[25-29] It has been reported by previous works that many conductive materials such as 2D (two-dimensional) materials,[8,30-32] nanowires,[9,33] metallic materials,[34-38] and polymer gel[10,39] are involved in fabrication of sensor electrodes. The pressure sensors with short period of response time have been focused on and shown promising application prospect, especially for the artificial intelligence. For instance, the pressure sensors based on a bioinspired porous dielectric layer between two ITO/PET electrodes, yield a rapid response time of 40 ms.[34] And it takes short time of approximately 63 ms for a CNT microyarn-based pressure sensor to identify applied pressures.[5] However, rare articles have pointed out that the flexible pressure sensors are able to detect dynamic changes of slight pressure with short intervals.

Recently, the main routes to enhance the responding performance of capacitive pressure sensors are changing conductive materials, transduction mechanism and encapsulation process. For the unique characteristics of its structure, the performance parameters of the capacitive pressure sensor are dominantly determined by two critical factors which are (1) the conductive material of two electrodes[33,40] and (2) the material and structure of dielectric

layer.[12,41] Referring to the dielectric layer, many complex models including micro-scale pyramids,[37,42-43] microporous structures[10,12,41] microdomes,[44] micro-pillar arrays,[45] rough interfaces[46] and other types[20] are proposed to boost the sensing sensitivity. However, fabrication of those kinds of microstructures requires intricate processes like traditional lithography and e-beam evaporation.[30,35] Moreover, some indispensable materials and devices such as Si mold,[42] photoresist and shadow mask,[47] nanowires,[34] Ecoflex[2] and polymer gel[10,39] increase the manufacturing costs and time. Therefore, a nylon netting widely used in the fabrication of solar battery[48] was first selected as an optimal material for a dielectric layer in our work, which reduces the costs as well as simplifies the manufacturing procedures. Additionally, the nylon netting mainly composed by PET (Polyethylene terephthalate) material shows regular microporous structure and eminent mechanical property, featuring our pressure sensors with high sensing sensitivity, long fatigue life and fast response speed.

Here, we propose a piezo-capacitive pressure sensor based on the elastic nylon-netting dielectric layer. The low-cost nylon netting layer with different thickness and mesh number insulates two graphene electrodes, providing the based pressure sensor with excellent pressure-sensing sensitivity of 0.33 kPa^{-1} under the pressure of 1 kPa, an ultralow detection limit of 3.3 Pa and outstanding mechanical stability after more than 1000 loading-unloading cycles. Furthermore, this sensor exhibits ultrafast response speed as 20 ms, which enables its detection for the small variations of applied pressures from the morphological changing processes of a falling droplet onto the sensor. Additionally, we reveal the promising applications of the pressure sensor in monitoring wrist pulse and answering mouse click. The

low-cost sensor arrays with excellent spatial resolution and response performance show great potential to be applied in the fields of electronic devices and wearable applications.

2. Results and discussion

Capacitive pressure sensors are fabricated by several processes, as illustrated in Figure 1a. A thin conductive layer of graphene (size: 18 × 8 mm^2) was first transferred onto PDMS-substrate (thickness: 650 μm, size: 30 × 30 mm^2) by PMMA-assisted method. Then, a silver wire with the diameter of 60 μm was connected by silver paint as the bottom electrode. Subsequently, a dielectric layer of nylon netting was covered onto the rest of the graphene electrode without air gap. Finally, the prepared structure was covered by another top graphene electrode, assembling a flexible sandwich-like capacitive pressure sensor. The size of the single graphene electrode without sliver paste is 16 × 13 mm^2 while the effective area of two face-to-face electrodes is 16 × 8 mm^2 after the complete of assembly. The Scanning electron microscope (SEM) image in Figure 1b shows that the graphene layer on the PDMS-substrate is homogenous. Raman spectra of graphene indicate high quality of the samples (Figure S1). Moreover, the sheet resistance of the graphene electrode is about 1~10 kΩ/□. The optical microscopy (OM) image shown in Figure 1c indicates that the graphene film on the flexible substrate is clean and flat over a large area. Three kinds of nylon-netting dielectric layers with different mesh number, thickness and size are demonstrated in Figure S2. Another OM image in Figure 1d shows that the nylon netting with a mesh number of 300 on the substrate is smooth, providing tremendously regular and uniform square holes. And

there are also clear dividing lines from top to bottom in Figure 1d. To assess the open-circuiting state and energy consumption of the pressure sensor, the changes of resistance R_{13} between two electrodes and R_{12} in two ends of top electrode under different loading pressure were recorded in Figure S3, which demonstrates the isolation of the sensor, because the R_{13} is at a very high magnitude of $\approx 10^9\ \Omega$, while the R_{12} is at the level of $\approx 10^4\ \Omega$.

Specifically, parameters of sensitivity, working stability, detection limit and response time are widely used to estimate the performance of pressure sensor.[40] The responding sensitivity S is a decisive factor to evaluate the operating performance of the sensor and defined as:

$$S = \frac{\delta(\Delta C / C_0)}{\delta p} \quad (1)$$

where C_0 and C are the capacitance without and with loading pressure, respectively. The relative change of capacitance is expressed by $\Delta C/C_0 = (C - C_0)/C_0$, and $\Delta C/C_0$ serves as a function of the applied pressure p and the slope represents the sensitivity. Based on our designed capacitive pressure sensor, it is clear that the dielectric layer consisting of nylon netting exerts an enormous function on the sensor's responding performance. Therefore, by altering the mesh number of nylon netting to regulate the thickness of dielectric layer, three kinds of nylon netting with different mesh number of 100, 200 and 300 were taken to optimize the pressure sensors. The size including thickness and length of the square hole of three nylon meshes are shown in Table S1. The impact of the different meshes in the pressure sensitivity was plotted in Figure 2a. The sensor based on 300-mesh nylon netting exhibits an improved sensitivity of 0.33 kPa^{-1} under the low-pressure working range (0-1 kPa) and 0.007

kPa^{-1} under the high-pressure working range (1-5 kPa). The sensitivity of other sensors based on 100-mesh and 200-mesh nylon netting were also calculated, as shown in Figure S4. As the mesh number of the nylon netting increases, the sensitivity of the sensors increases. But, when the mesh number is increased to 420, the capacitance change of the sensor is less than that of sensors based on 200-mesh and 300-mesh nylon netting under the same pressure (Figure S5). Therefore, there is a turning point that excessive mesh numbers of nylon netting impact negative effects on the performance of pressure sensor. Owing to the high Poisson ratio (0.47) and Young's Modulus (600 kPa) modulus of the PDMS-substrate,[40,49] the capacitance response of all these sensors rises sharply at the low-pressure range and changes slightly at the high-pressure range with the increasing pressure. The sensitivity of our fabricated sensors is comparable with the capacitive sensors previously.[5,10,44-45,50]

For comparing the responding capability, capacitive pressure sensors based on 100-mesh, 200-mesh and 300-mesh nylon netting are subjected to a certain pressure of 500 Pa, as exhibited in Figure 2b, showing noticeable capacitance responses of 36%, 78% and 108%, respectively. Considering the preferable sensing actions from the pressure sensor based on 300-mesh nylon netting, a nearly linear pressure was applied to inspect the sensing ability of the sensor. Figure 2c shows stable capacitance responses under pressure and returns to its off state after removing the pressure. To investigate the restorability of the sensor, a typical loading-unloading cycle is shown in Figure 2d, indicating that the sensing curve of the unloading process of the pressure is in good agreement with that during the loading process. And the response of the sensor returns to zero after removing the pressure. The tiny hysteresis

between loading and unloading curve is due to the viscoelasticity of thin PDMS-substrate. A further restorative test was conducted by applying stepped pressure on the pressure senor, which leads to corresponding capacitance responses and demonstrates its outstanding pressure identifiability, as shown in Figure 2e. And the pressure sensor restored to its initial state in short time after the removal of the applied pressure, which shows the favorable recoverability. Our pressure sensors also exhibit long fatigue life. The relative capacitance variations remained stable after 1050 loading-unloading cycles under 400 and 1000 Pa respectively, as illustrated in Figure 2f and S6. The capacitance responses of the pressure sensor still reach to 82% and 125% under two applied pressures respectively, after 30-min loading-unloading cycles, as shown in two insets of Figure 2f. Additionally, when the same pressure is applied on the pressure sensor at different local places chosen randomly, the capacitance responses keep stable (Figure S7), which demonstrates its positional indifference for pressure detection.

The ability to detect ultralow pressure is also very important for the capacitive pressure sensor. A distinguishable capacitance variation in Figure 3a results from the loading and removal of a light butterfly, which generates a tiny pressure of ≈ 3.3 Pa. For evaluating the practical behavior in sensing ultralight objects, a staple was horizontally or vertically placed on the pressure sensor, respectively that triggers to two distinctly different capacitance responses, as shown in Figure 3b. Due to different contacting areas of the same staple, it generates pressure with different values applying on the sensor. To verify the fast response speed of the sensor for dynamic pressure, a sequence of liquid droplets was drop on the

sensor. In Figure 3c, the stepped escalation of the capacitance response is primarily associated with the accumulation process of four water droplets on the sensor. Furthermore, it is worth noticing the damped oscillation at the starting of each step, one of which is marked by the black circle in Figure 3c and enlarged in Figure 3d. It is reasonable to think that the oscillation is attributed to the elastic interaction between the droplet and the pressure sensor, which leads to the dynamic change of the applied pressure until the water droplet keeps steady. The process can be separated to four parts as marked by numbers in Figure 3d, each of them was recorded by a high-speed camera. Specifically, Figure 3e-① shows the falling process of a water droplet from a dropper due to the gravity, during which the droplet acquires momentum and kinetic energy. After touching the pressure sensor, the gravity and the momentum of the droplet jointly generated a compression and led to the morphological change of the droplet, which is shown in Figure 3e-② and corresponds to the maximum response in Figure 3d-②. Subsequently, the aggregation state of the droplet in Figure 3e-③ indicates that the electrode combined with the water droplet bounced upward owing to the elastic potential energy induced by the electrode deformation. Thus, the corresponding capacitance response shown in Figure 3d-③ falls down to a minimum point. The consecutive elastic interaction and the capacitance variations reached a relatively stable state because the elastic potential energy running out after a short time ≈ 1s. In this stage, a stable response value can be observed in Figure 3d-④ with a practically unchanging state of the droplet in Figure 3e-④. According to the capacitance response shown in Figure 3d and the interval between the captured photographs Figure 3e-① and 3e-②, the response time of the

pressure sensor is less than 20 ms.

For convenient applications in human-health monitoring, the capacitive pressure sensor based on 100-mesh nylon netting was adhered onto the wrist of a volunteer to monitor wrist pulse via a scotch tape. The pressure-sensing signals are presented in Figure 4a, which are clearly in good agreement with the frequency (~ 1Hz) of human wrist pulse. Therefore, the sensor shows promising potential to detect weak biomedical signals. Furthermore, the high sensitivity for human touch and fast response speed assure that it is also suitable to be applied in mouse keys. In Figure 4b, the pressure sensor based on 300-mesh nylon netting exhibits stable and synchronous responses to consecutive human clicks. It is also competent to identify double clicks with the interval of hundreds of microseconds, as shown in Figure S8. A single capacitive sensor is able to detect applied pressure but without spatial resolution. It is reported previously that capacitive sensor array units optimize the responding performance as well as spatial resolution under pressure[28,40,41,43] for application in biomedical diagnosis and wearable devices, such as computer keyboard and human-motion detector.[11-12,46,50] Figure 4c shows a 4 × 4 multipixel sensor array based on 300-mesh nylon netting, the size of which is 20×20 mm^2. The schematics of the fabrication process of the sensor array are illustrated in Figure S9. For testing the spatial pressure resolution, a blue steel ball (500 mg) was placed on the unit 2B with a loading pressure of 250 Pa of the sensor array, as shown in Figure 4c. A 3D (three-dimensional) distribution graph in Figure 4d clarifies that the highest capacitance response located at the unit 2B, where the blue steel ball was placed. Simultaneously, other adjacent units including 1B, 2A, 2C and 3B also show small capacitance variations, which is

ascribed to the spreading deformation from the unit 2B under the gravity of the steel. And the adjacent units have an offset of approximately 6.0 %. Because the diameter of the blue steel ball is 5 mm, which is very close to the size of the unit 2B with the area of 5 × 5 mm^2, and the ball was not exactly placed at the pinpoint of center unit 2B. Another experiment has been implemented that a cylindrical indenter with a much smaller bottom diameter of 1 mm is used to apply pressure on the unit 2B, the adjacent units of which have a similar offset of less than 6.0%, as shown in Figure S10.

The comprehensive sensing performance of the pressure sensor based on the piezo-capacitive effect is closely interrelated with its working mechanism, which is interpreted in Figure 5. For avoiding an imperfect performance owing to the adhesiveness of flexible substrate, a thin nylon-netting dielectric layer composed by the PET material mainly serves as the function layer for optimization of the pressure sensor. Considering the special microporous structure of the dielectric layer and the preferable flexibility of the electrode, the sensor can easily achieve definite deformation with the compression of air gap between two electrodes under loading pressure, which increases the effective area A slightly but decreases the effective distance d evidently owing to the high Young's Modulus (600 kPa) and Poisson ratio (0.47) of PDMS-substrate.[40,49] Based on the structure of the sensor, the capacitance of the sensor without (C_0) and with (C) applied pressure can be expressed by:

$$C_0 = \frac{\varepsilon_{air} A_{air} + \varepsilon_{NN} A_{NN}}{d^0} \quad (2)$$

$$C = \frac{\varepsilon_{air} A'_{air}}{d'} + \frac{\varepsilon_{NN} A_{NN}}{d^0} \quad (3)$$

Where ε_{air} and ε_{NN} are the permittivity of air and dielectric layer respectively, A_{air} and A_{NN} are

the effective area of air gap within the square holes of dielectric layer and remaining areas of dielectric layer respectively. $A^{'}_{air}$ is the effective area of the air gap under the applied pressure. d^0 and $d^{'}$ is the effective distance of two electrodes without and with loading pressure respectively. Accordingly, the capacitance response $\Delta C/C_0$ is calculated by:

$$\frac{\Delta C}{C_0} = \frac{C - C_0}{C_0} = \frac{\varepsilon_{air} d^0 A^{'}_{air} - \varepsilon_{air} d^{'} A_{air}}{\varepsilon_{air} d^{'} A_{air} + \varepsilon_{NN} d^{'} A_{NN}} \quad (4)$$

Therefore, distinguishable and rapid capacitance responses to the applied pressure of the sensor based on the sandwich-like structure demonstrate that the valid changes of A and d with a stable ε are optimal factors for promoting the capacitance variation and pressure sensitivity. In addition, it is feasible to modify the size of the porous dielectric layer and pore distribution to tune the performance of based pressure sensors.

3. Conclusions

In summary, we developed facile capacitive pressure sensors based on the handy and cost-effective nylon netting with microscale and regularly distributed square holes via a high-efficiency and low-cost process. The capacitive pressure sensor shows a high sensitivity up to 0.33 kPa^{-1} in a low-pressure sensing range, excellent mechanical stability, long working durability under 400 and 1000 Pa over 1050 repeating cycles, and ultralow detection limit less than 3.3 Pa. Our designed pressure sensors are also able to detect pulse signals in real time as well as identify human clicks for application in mouse keys. Meaningfully, the simply-structured pressure sensor has fast response capability of 20 ms. The combination of high sensitivity and fast response speed of the sensor facilitates its identification for

dynamically changing pressure, such as the momentum transformation processes of a water droplet drop on the sensor. Furthermore, a capacitive pressure sensor array with 4 × 4 multipixel shows high pressure spatial resolution, which meets the requirements to practical application. We believe that this sandwich-like flexible pressure sensor with high sensitivity, brilliant stability and dynamic detecting capability is an applicable candidate for wearable devices and biomedical monitoring.

4. Experimental Section

Preparation of Graphene: Graphene was grown on the copper foil (thickness: 0.025 mm) by the method of CVD, as reported by our previous work.[15,51-52] First, the copper foil substrate was cut into suitable size and then put in the tubular furnace. Then, the tubular furnace was heated to 1010 °C in 40 min under the environment of Ar (200 sccm) and H_2 (80 sccm) and keep annealing the growth substrate for 30 min. Subsequently, CH_4 (30 sccm) was introduced into the tubular furnace for 5-8 min for synthesis of graphene, followed by pulling the copper foil substrate out from the reaction zone rapidly for cooling down to ambient temperature under the protection atmosphere of Ar (200 sccm) and H_2 (80 sccm).

Transfer of Graphene: A thin PMMA (mass fraction: 5%) film was coated on the grown graphene in previous step and dried in the electrothermal blowing oven for 30 min. Then, the dried sample was put onto the surface of 0.5 M $FeCl_3$ solution to etch the copper foil substrate for 50-60 min, proceeded by transferring the floated graphene with the PMMA onto the surface of deionized water (DI) water for several times to eliminate the remaining

contaminants. Subsequently, a PDMS-substrate with the thickness of 650 μm (Sylgard184: Dow Corning =10:1) was first treated well by air plasma for 3 min to increase its hydrophilicity and the floated graphene with clean PMMA film was transferred onto the prepared PDMS-substrate and dried in an oven for 30-40 min. The dried sample was finally soaked into an acetone solution heated at 50 °C to remove the PMMA, and the clean graphene on the PDMS-substrate was obtained.

Processing of Nylon Netting: A customized nylon netting was first flattened using the definite pre-pressure and cut into desirable size for convenient assembling. The as-prepared nylon netting was closely fixed on the graphene electrode in the previous step by a scotch tape to prevent the dielectric layer from moving or slipping in the assembling process and avoid the adverse effect of the gap between the electrode and dielectric layer.

Fabrication of Capacitive Sensor Array: Clean and homogenous graphene electrodes of pressure sensor array were first prepared by the above steps. Subsequently, the graphene film on PDMS-substrate was fixed on a horizontal mechanical motion stage, followed by cutting into applicable size for ideal graphene electrode stripes via the high-energy laser of a Avia 266 nm Solid State Q-Switched UV Laser (energy: 0.14W). A nylon netting was then closely fixed on the ready-made graphene electrode stripes, which was orthogonally covered by another graphene electrode stripes assembling a facile 4 × 4 capacitive pressure sensor array.

Structural Characterization and Performance Measurement of Pressure Sensors: SEM images were captured using a Scanning Electron Microscope (Hitachi S- 4800) with the operating voltage of 5 kV. Optical microscopy images were captured using an Optical

Microscope (Zeiss Axio CSM 700). Raman spectra were measured by a Raman spectrometer (HORIBA JY HR800) with 633 nm excitation laser. The sheet resistance of the graphene electrode was measured by a RTS-9 four-point probes Resistivity Measurement System. The ever-changing process of a droplet falling from above the pressure sensor till touching was captured using a high-speed camera (PCO.1200 s/hs) with an image corresponding to 10 ms. The capacitance was measured by An Agilent E4980A LCR meter with the performance in Figure 2 at a frequency of 1 kHz and the practical applications in Figure 3 and 4 at a frequency of 300 kHz using a 1V AC voltage, which was recorded via a Labview program. The mechanical pressure was provided and recorded by a mechanical motion controller (Zolix SC300-3A, 1.25 μm resolution) and a force gauge (Mark 10, 0.1 mN resolution) on a stable experiment platform, which were driven by a computer.

Acknowledgements

This work was financially supported by National Natural Science Foundation of China (Grant No. 51772335), Guangdong Natural Science Foundation (Grant No. 2016A030313346 and 2014A030306022), Guangdong Youth Top-notch Talent Support Program (No. 2015TQ01C201).

Supporting Information

Raman spectra of Graphene, OM images and parameters of three kinds of nylon netting, the resistance variations of the electrodes, sensitivity and stability of the sensors based on the

three kinds of nylon netting. The Supporting Information is available free of charge on the ACS Publications website.

References

(1) Chen, D.; Pei, Q. Electronic Muscles and Skins: A Review of Soft Sensors and Actuators. *Chem. Rev.* **2017**, *117*, 11239–11268.

(2) Gerratt, A. P.; Michaud, H. O.; Lacour, S. P. Elastomeric Electronic Skin for Prosthetic Tactile Sensation. *Adv. Funct. Mater.* **2015**, *25*, 2287–2295.

(3) Choi, S.; Lee, H.; Ghaffari, R.; Hyeon, T.; Kim, D. H. Recent Advances in Flexible and Stretchable Bio-Electronic Devices Integrated with Nanomaterials. *Adv. Mater.* **2016**, *28*, 4203–4218.

(4) Khan, Y.; Ostfeld, A. E.; Lochner, C. M.; Pierre, A.; Arias, A. C. Monitoring of Vital Signs with Flexible and Wearable Medical Devices. *Adv. Mater.* **2016**, *28*, 4373–4395.

(5) Kim, S. Y.; Park, S.; Park, H. W.; Park, D. H.; Jeong, Y.; Kim, D. H. Highly Sensitive and Multimodal All-Carbon Skin Sensors Capable of Simultaneously Detecting Tactile and Biological Stimuli. *Adv. Mater.* **2015**, *27*, 4178–4185.

(6) Gao, Y.; Ota, H.; Schaler, E. W.; Chen, K.; Zhao, A.; Gao, W.; Fahad, H. M.; Leng, Y.; Zheng, A.; Xiong, F.; Zhang, C.; Tai, L. C.; Zhao, P.; Fearing, R. S.; Javey, A. Wearable Microfluidic Diaphragm Pressure Sensor for Health and Tactile Touch Monitoring. *Adv. Mater.* **2017**, *29*, 1701985.

(7) Liu, Q.; Chen, J.; Li, Y.; Shi, G. High-Performance Strain Sensors with Fish-Scale-Like

Graphene-Sensing Layers for Full-Range Detection of Human Motions. *ACS Nano* **2016**, *10*, 7901–7906.

(8) Kang, M.; Kim, J.; Jang, B.; Chae, Y.; Kim, J. H.; Ahn, J. H. Graphene-Based Three-Dimensional Capacitive Touch Sensor for Wearable Electronics. *ACS Nano* **2017**, *11*, 7950–7957.

(9) Kim, S. R.; Kim, J. H.; Park, J. W. Wearable and Transparent Capacitive Strain Sensor with High Sensitivity Based on Patterned Ag Nanowire Networks. *ACS Appl. Mater. Interfaces* **2017**, *9*, 26407–26416.

(10) Yoon, S. G.; Park, B. J.; Chang, S. T. Highly Sensitive Piezocapacitive Sensor for Detecting Static and Dynamic Pressure Using Ion-Gel Thin Films and Conductive Elastomeric Composites. *ACS Appl. Mater. Interfaces* **2017**, *9*, 36206-36219.

(11) Chen, S.; Zhuo, B.; Guo, X. Large Area One-Step Facile Processing of Microstructured Elastomeric Dielectric Film for High Sensitivity and Durable Sensing over Wide Pressure Range. *ACS Appl. Mater. Interfaces* **2016**, *8*, 20364–20370.

(12) Li, T.; Luo, H.; Qin, L.; Wang, X.; Xiong, Z.; Ding, H.; Gu, Y.; Liu, Z.; Zhang, T. Flexible Capacitive Tactile Sensor Based on Micropatterned Dielectric Layer. *Small* **2016**, *12*, 5042–5048.

(13) Chen, Y.-M.; He, S.-M.; Huang, C.-H.; Huang, C.-C.; Shih, W.-P.; Chu, C.-L.; Kong, J.; Li, J.; Su, C.-Y. Ultra-Large Suspended Graphene as a Highly Elastic Membrane for Capacitive Pressure Sensors. *Nanoscale* **2016**, *8*, 3555–3564.

(14) Davidovikj, D.; Scheepers, P. H.; van der Zant, H. S. J.; Steeneken, P. G. Static

Capacitive Pressure Sensing Using a Single Graphene Drum. *ACS Appl. Mater. Interfaces* **2017**, *9*, 43205-43210.

(15) Chen, W.; Gui, X.; Liang, B.; Yang, R.; Zheng, Y.; Zhao, C.; Li, X.; Zhu, H.; Tang, Z. Structural Engineering for High Sensitivity, Ultrathin Pressure Sensors Based on Wrinkled Graphene and Anodic Aluminum Oxide Membrane. *ACS Appl. Mater. Interfaces* **2017**, *9*, 24111–24117.

(16) Lou, Z.; Chen, S.; Wang, L.; Jiang, K.; Shen, G. An Ultra-Sensitive and Rapid Response Speed Graphene Pressure Sensors for Electronic Skin and Health Monitoring. *Nano Energy* **2016**, *23*, 7–14.

(17) Liang, B.; Chen, W.; He, Z.; Yang, R.; Lin, Z.; Du, H.; Shang, Y.; Cao, A.; Tang, Z.; Gui, X. Highly Sensitive, Flexible MEMS Based Pressure Sensor with Photoresist Insulation Layer. *Small* **2017**, *13*, 1702422.

(18) Liu, S.; Wu, X.; Zhang, D.; Guo, C.; Wang, P.; Hu, W.; Li, X.; Zhou, X.; Xu, H.; Luo, C.; Zhang, J.; Chu, J. Ultrafast Dynamic Pressure Sensors Based on Graphene Hybrid Structure. *ACS Appl. Mater. Interfaces* **2017**, *9*, 24148–24154.

(19) Zhong, H.; Xia, J.; Wang, F.; Chen, H.; Wu, H.; Lin, S. Graphene-Piezoelectric Material Heterostructure for Harvesting Energy from Water Flow. *Adv. Funct. Mater.* **2017**, *27*, 1604226.

(20) Lee, J. H.; Yoon, H. J.; Kim, T. Y.; Gupta, M. K.; Lee, J. H.; Seung, W.; Ryu, H.; Kim, S. W. Micropatterned P(VDF-TrFE) Film-Based Piezoelectric Nanogenerators for Highly Sensitive Self-Powered Pressure Sensors. *Adv. Funct. Mater.* **2015**, *25*, 3203–3209.

(21) Kong, D.; Pfattner, R.; Chortos, A.; Lu, C.; Hinckley, A. C.; Wang, C.; Lee, W. Y.; Chung, J. W.; Bao, Z. Capacitance Characterization of Elastomeric Dielectrics for Applications in Intrinsically Stretchable Thin Film Transistors. *Adv. Funct. Mater.* **2016**, *26*, 4680–4686.

(22) Schwartz, G.; Tee, B. C. K.; Mei, J.; Appleton, A. L.; Kim, D. H.; Wang, H.; Bao, Z. Flexible Polymer Transistors with High Pressure Sensitivity for Application in Electronic Skin and Health Monitoring. *Nat. Commun.* **2013**, *4*, 1858–1859.

(23) Lin, L.; Xie, Y.; Wang, S.; Wu, W.; Niu, S.; Wen, X.; Wang, Z. L. Triboelectric Active Sensor Array for Self-Powered Static and Dynamic Pressure Detection and Tactile Imaging. *ACS Nano* **2013**, *7*, 8266–8274.

(24) Yao, H. Bin; Ge, J.; Wang, C. F.; Wang, X.; Hu, W.; Zheng, Z. J.; Ni, Y.; Yu, S. H. A Flexible and Highly Pressure-Sensitive Graphene-Polyurethane Sponge Based on Fractured Microstructure Design. *Adv. Mater.* **2013**, *25*, 6692–6698.

(25) Pang, C.; Lee, G.-Y.; Kim, T.; Kim, S. M.; Kim, H. N.; Ahn, S.-H.; Suh, K.-Y. A Flexible and Highly Sensitive Strain-Gauge Sensor Using Reversible Interlocking of Nanofibres. *Nat. Mater.* **2012**, *11*, 795–801.

(26) Yao, S.; Zhu, Y. Wearable Multifunctional Sensors Using Printed Stretchable Conductors Made of Silver Nanowires. *Nanoscale* **2014**, *6*, 2345-2352.

(27) Park, S.; Kim, H.; Vosgueritchian, M.; Cheon, S.; Kim, H.; Koo, J. H.; Kim, T. R.; Lee, S.; Schwartz, G.; Chang, H.; Bao, Z. Stretchable Energy-Harvesting Tactile Electronic Skin Capable of Differentiating Multiple Mechanical Stimuli Modes. *Adv. Mater.* **2014**, *26*,

7324–7332.

(28) Zhao, X.; Hua, Q.; Yu, R.; Zhang, Y.; Pan, C. Flexible, Stretchable and Wearable Multifunctional Sensor Array as Artificial Electronic Skin for Static and Dynamic Strain Mapping. *Adv. Electron. Mater.* **2015**, *1*, 1500142.

(29) Sheng, L.; Liang, Y.; Jiang, L.; Wang, Q.; Wei, T.; Qu, L.; Fan, Z. Bubble-Decorated Honeycomb-Like Graphene Film as Ultrahigh Sensitivity Pressure Sensors. *Adv. Funct. Mater.* **2015**, *25*, 6545–6551.

(30) Wang, X.; Li, T.; Adams, J.; Yang, J. Transparent, Stretchable, Carbon-Nanotube-Inlaid Conductors Enabled by Standard Replication Technology for Capacitive Pressure, Strain and Touch Sensors. *J. Mater. Chem. A* **2013**, *1*, 3580-3586.

(31) Wan, S.; Bi, H.; Zhou, Y.; Xie, X.; Su, S.; Yin, K.; Sun, L. Graphene Oxide as High-Performance Dielectric Materials for Capacitive Pressure Sensors. *Carbon* **2017**, *114*, 209–216.

(32) Lipomi, D. J.; Vosgueritchian, M.; Tee, B. C.-K.; Hellstrom, S. L.; Lee, J. A.; Fox, C. H.; Bao, Z. Skin-like Pressure and Strain Sensors Based on Transparent Elastic Films of Carbon Nanotubes. *Nat. Nanotechnol.* **2011**, *6*, 788–792.

(33) Joo, Y.; Byun, J.; Seong, N.; Ha, J.; Kim, H.; Kim, S.; Kim, T.; Im, H.; Kim, D.; Hong, Y. Silver Nanowire-Embedded PDMS with a Multiscale Structure for a Highly Sensitive and Robust Flexible Pressure Sensor. *Nanoscale* **2015**, *7*, 6208–6215.

(34) Kang, S.; Lee, J.; Lee, S.; Kim, S. G.; Kim, J. K.; Algadi, H.; Al-Sayari, S.; Kim, D. E.; Kim, D. E.; Lee, T. Highly Sensitive Pressure Sensor Based on Bioinspired Porous Structure

for Real-Time Tactile Sensing. *Adv. Electron. Mater.* **2016**, *2*, 1600356.

(35) Vandeparre, H.; Watson, D.; Lacour, S. P. Extremely Robust and Conformable Capacitive Pressure Sensors Based on Flexible Polyurethane Foams and Stretchable Metallization. *Appl. Phys. Lett.* **2013**, *103*, 204103.

(36) Pan, L.; Chortos, A.; Yu, G.; Wang, Y.; Isaacson, S.; Allen, R.; Shi, Y.; Dauskardt, R.; Bao, Z. An Ultra-Sensitive Resistive Pressure Sensor Based on Hollow-Sphere Microstructure Induced Elasticity in Conducting Polymer Film. *Nat. Commun.* **2014**, *5*, 3002.

(37) Mannsfeld, S. C. B.; Tee, B. C.-K.; Stoltenberg, R. M.; Chen, C. V. H.-H.; Barman, S.; Muir, B. V. O.; Sokolov, A. N.; Reese, C.; Bao, Z. Highly Sensitive Flexible Pressure Sensors with Microstructured Rubber Dielectric Layers. *Nat. Mater.* **2010**, *9*, 859–864.

(38) Viry, L.; Levi, A.; Totaro, M.; Mondini, A.; Mattoli, V.; Mazzolai, B.; Beccai, L. Flexible Three-Axial Force Sensor for Soft and Highly Sensitive Artificial Touch. *Adv. Mater.* **2014**, *26*, 2659–2664.

(39) Lei, Z.; Wang, Q.; Sun, S.; Zhu, W.; Wu, P. A Bioinspired Mineral Hydrogel as a Self-Healable, Mechanically Adaptable Ionic Skin for Highly Sensitive Pressure Sensing. *Adv. Mater.* **2017**, *29*, 1700321.

(40) Shuai, X.; Zhu, P.; Zeng, W.; Hu, Y.; Liang, X.; Zhang, Y.; Sun, R.; Wong, C. P. Highly Sensitive Flexible Pressure Sensor Based on Silver Nanowires-Embedded Polydimethylsiloxane Electrode with Microarray Structure. *ACS Appl. Mater. Interfaces* **2017**, *9*, 26314–26324.

(41) Kwon, D.; Lee, T. I.; Shim, J.; Ryu, S.; Kim, M. S.; Kim, S.; Kim, T. S.; Park, I.

Highly Sensitive, Flexible, and Wearable Pressure Sensor Based on a Giant Piezocapacitive Effect of Three-Dimensional Microporous Elastomeric Dielectric Layer. *ACS Appl. Mater. Interfaces* **2016**, *8*, 16922–16931.

(42) Zhang, X.; Hu, S.; Wang, M.; Yu, J.; Khan, Q.; Shang, J.; Ba, L. Continuous Graphene and Carbon Nanotube Based High Flexible and Transparent Pressure Sensor Arrays. *Nanotechnology* **2015**, *26*, 115501.

(43) Boutry, C. M.; Nguyen, A.; Lawal, Q. O.; Chortos, A.; Rondeau-Gagné, S.; Bao, Z. A Sensitive and Biodegradable Pressure Sensor Array for Cardiovascular Monitoring. *Adv. Mater.* **2015**, *27*, 6954–6961.

(44) Miller, S.; Bao, Z. Fabrication of Flexible Pressure Sensors with Microstructured Polydimethylsiloxane Dielectrics Using the Breath Figures Method. *J. Mater. Res.* **2015**, *30*, 3584–3594.

(45) Pang, C.; Koo, J. H.; Nguyen, A.; Caves, J. M.; Kim, M. G.; Chortos, A.; Kim, K.; Wang, P. J.; Tok, J. B. H.; Bao, Z. Highly Skin-Conformal Microhairy Sensor for Pulse Signal Amplification. *Adv. Mater.* **2015**, *27*, 634–640.

(46) Lee, K.; Lee, J.; Kim, G.; Kim, Y.; Kang, S.; Cho, S.; Kim, S.; Kim, J. K.; Lee, W.; Kim, D. E.; Kang, S.; Kim, D.; Lee, T.; Shim, W. Rough-Surface-Enabled Capacitive Pressure Sensors with 3D Touch Capability. *Small* **2017**, *13*, 1700368.

(47) Woo, S.-J.; Kong, J.-H.; Kim, D.-G.; Kim, J.-M. A Thin All-Elastomeric Capacitive Pressure Sensor Array Based on Micro-Contact Printed Elastic Conductors. *J. Mater. Chem. C* **2014**, *2*, 4415–4422.

(48) Krebs, F. C.; Fyenbo, J.; Jørgensen, M. Product Integration of Compact Roll-to-Roll Processed Polymer Solar Cell Modules: Methods and Manufacture Using Flexographic Printing, Slot-Die Coating and Rotary Screen Printing. *J. Mater. Chem.* **2010**, *20*, 8994-9001.

(49) Okatani, T.; Takahashi, H.; Noda, K.; Takahata, T.; Matsumoto, K.; Shimoyama, I. A Tactile Sensor Using Piezoresistive Beams for Detection of the Coefficient of Static Friction. *Sensors* **2016**, *16*, 718-728.

(50) Lee, J.; Kwon, H.; Seo, J.; Shin, S.; Koo, J. H.; Pang, C.; Son, S.; Kim, J. H.; Jang, Y. H.; Kim, D. E.; Lee, T. Conductive Fiber-Based Ultrasensitive Textile Pressure Sensor for Wearable Electronics. *Adv. Mater.* **2015**, *27*, 2433–2439.

(51) Chen, W.; Gui, X.; Zheng, Y.; Liang, B.; Lin, Z.; Zhao, C.; Chen, H.; Chen, Z.; Li, X.; Tang, Z. Synergistic Effects of Wrinkled Graphene and Plasmonics in Stretchable Hybrid Platform for Surface-Enhanced Raman Spectroscopy. *Adv. Opt. Mater.* **2017**, *5*, 1600715.

(52) Chen, W.; Gui, X.; Liang, B.; Liu, M.; Lin, Z.; Zhu, Y.; Tang, Z. Controllable Fabrication of Large-Area Wrinkled Graphene on a Solution Surface. *ACS Appl. Mater. Interfaces* **2016**, *8*, 10977–10984.

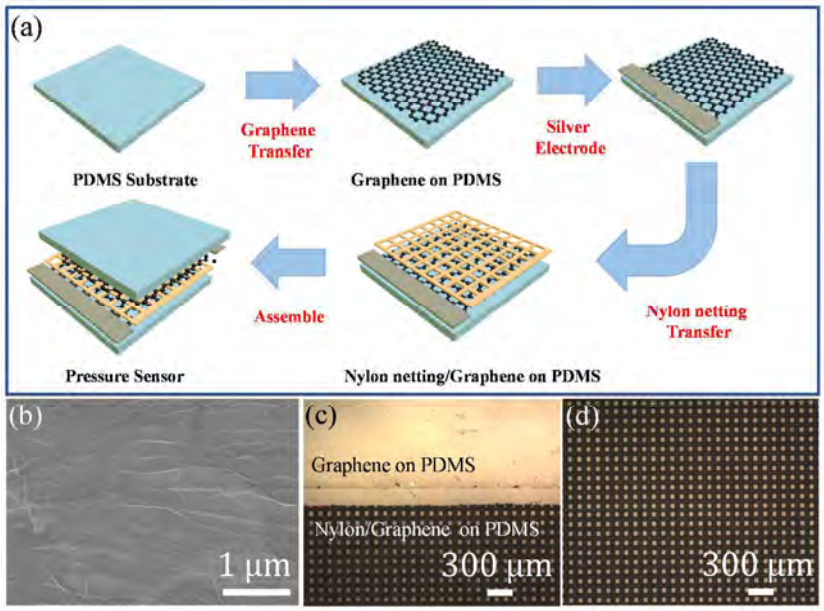

Figure 1. The fabrication processes and structural characterization of capacitive pressure sensor. (a) The fabrication steps of the sandwich-like pressure sensor based on a low-cost nylon netting with numerous microsized square holes. (b) SEM image of graphene on PDMS substrate. (c) OM image of nylon netting/graphene on PDMS substrate. (d) OM image of nylon netting on PDMS substrate.

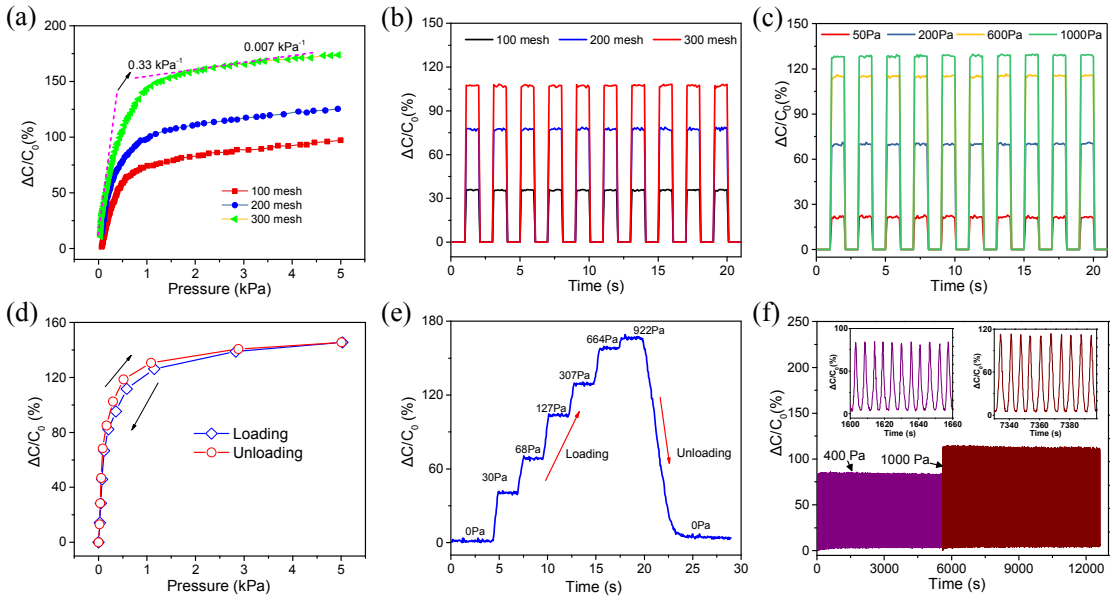

Figure 2. Pressure responding capabilities of the capacitive pressure sensor base on a handy Nylon netting. (a) Pressure-sensing sensitivity curves of pressure sensors based on three nylon nettings with different mesh numbers. (b) Capacitance responses of pressure sensors based on three nylon nettings with different mesh numbers under a pressure of 500 Pa. (c) Capacitance responses of the pressure sensor based on 300-mesh nylon netting under various applied pressures. (d) Capacitance responses of the pressure sensor based on 300-mesh nylon netting in a loading-unloading cycle. (e) Capacitance responses of the pressure sensor based on 300-mesh nylon netting under the half-step loading-unloading pressure circumstances. (f) Working stability and durability of the pressure sensor response after 1050 cycles under the applied pressures of 400 and 1000 Pa, respectively. And two insets are the capacitance responses after 30-min test under 400 and 1000 Pa respectively.

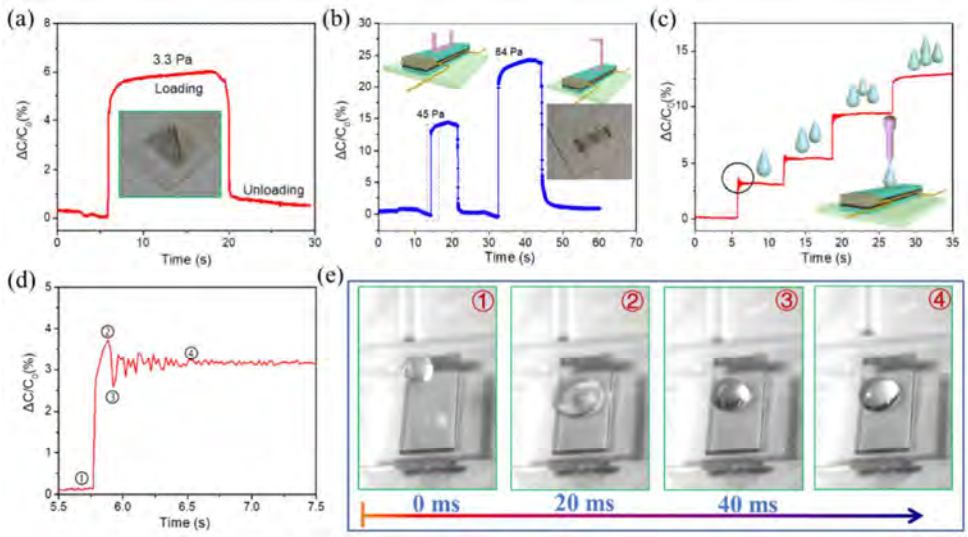

Figure 3. Pressure-sensing performances of the capacitive pressure sensors under the pressure of objects. (a) Capacitance response of the pressure sensor based on 300-mesh nylon netting to the loading and removing of a butterfly (≈ 22 mg). (b) Capacitance responses of the pressure sensor to a staple (≈ 81 mg) with two contact interfaces. (c) Capacitance responses of the pressure sensor to the fallen droplet (≈ 20 mg) with an applied pressure of approximately 7 Pa. (d) Capacitance responses of the pressure sensor to the dynamic changes of applied pressure generated by the fallen droplet, which is in correspondence to the part of the curve marked by a black circle in (c). (e) Photographs of the ultrafast and tiny form changes of the fallen droplet on the sensor.

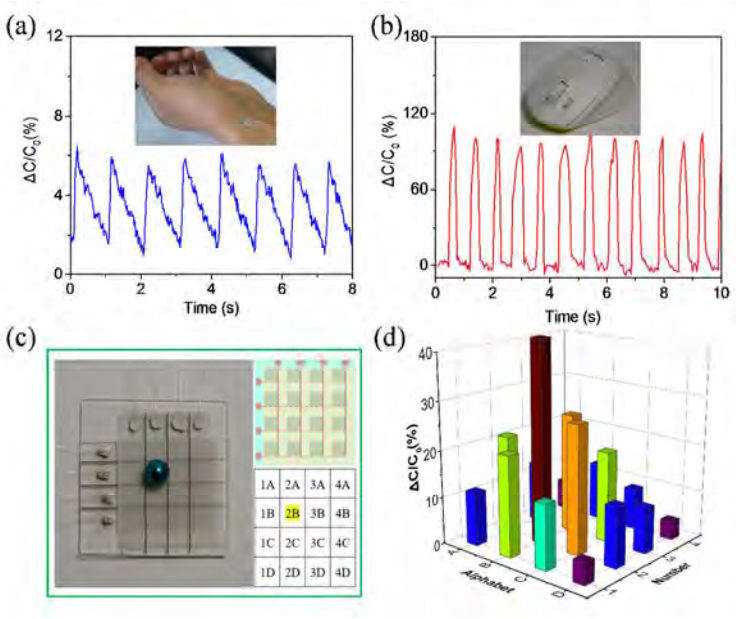

Figure 4. The practical applications and integrated array of the capacitive pressure sensor. (a) Real-time surveillance of the pressure sensor for the wrist pulses. (b) Application of the pressure sensor for mouse keys. (c) Image of a 4 × 4 pressure sensor array with loading a blue steel on unit 2B. (d) The corresponding responses with spatial distribution of (c).

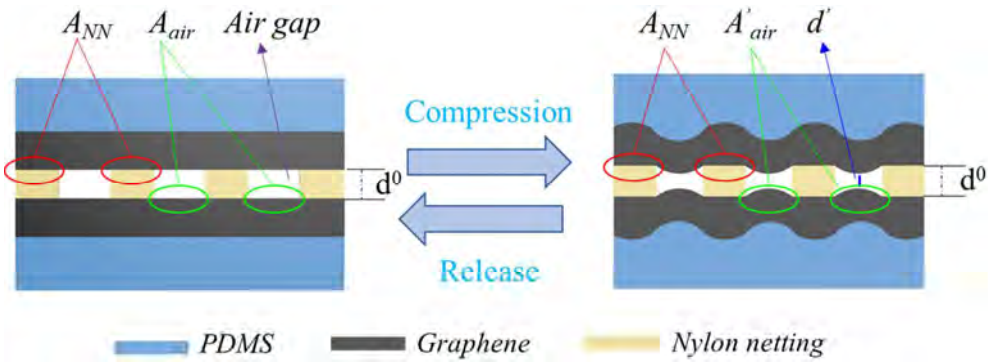

Figure 5. The schematic diagrams of the operating mechanism of the capacitive pressure sensor.

Table of Contents